Forced Hepatic Overexpression of CEACAM1 Curtails Diet-Induced Insulin Resistance

Qusai Y. Al-Share,[1,2] Anthony M. DeAngelis,[1,2] Sumona Ghosh Lester,[1,2] Thomas A. Bowman,[1,2] Sadeesh K. Ramakrishnan,[1,2] Simon L. Abdallah,[1,2] Lucia Russo,[1,2] Payal R. Patel,[1,2] Meenakshi K. Kaw,[1,2] Christian K. Raphael,[1,2] Andrea Jung Kim,[1,3] Garrett Heinrich,[1,3] Abraham D. Lee,[1,3] Jason K. Kim,[4] Rohit N. Kulkarni,[5] William M. Philbrick,[6] and Sonia M. Najjar[1,2]

Forced Hepatic Overexpression of CEACAM1 Curtails Diet-Induced Insulin Resistance

Diabetes 2015;64:2780–2790 | DOI: 10.2337/db14-1772

Carcinoembryonic antigen-related cell adhesion molecule 1 (CEACAM1) regulates insulin sensitivity by promoting hepatic insulin clearance. Liver-specific inactivation or global null-mutation of *Ceacam*1 impairs hepatic insulin extraction to cause chronic hyperinsulinemia, resulting in insulin resistance and visceral obesity. In this study we investigated whether diet-induced insulin resistance implicates changes in hepatic CEACAM1. We report that feeding C57/BL6J mice a high-fat diet reduced hepatic CEACAM1 levels by >50% beginning at 21 days, causing hyperinsulinemia, insulin resistance, and elevation in hepatic triacylglycerol content. Conversely, liver-specific inducible CEACAM1 expression prevented hyperinsulinemia and markedly limited insulin resistance and hepatic lipid accumulation that were induced by prolonged high-fat intake. This was partly mediated by increased hepatic β-fatty acid oxidation and energy expenditure. The data demonstrate that the high-fat diet reduced hepatic CEACAM1 expression and that overexpressing CEACAM1 in liver curtailed diet-induced metabolic abnormalities by protecting hepatic insulin clearance.

Insulin resistance, the hallmark of metabolic diseases, is commonly heralded by hyperinsulinemia. The cause-and-effect relationship between chronic hyperinsulinemia and reduced insulin response remains somewhat elusive but has received renewed interest (1–3). Peripheral insulin resistance induces compensatory insulin secretion, resulting in hyperinsulinemia. Reciprocally, hyperinsulinemia causes insulin resistance via mechanisms including down-regulating insulin receptors (4) and promoting hepatic de novo lipogenesis, in part, by activating the sterol regulatory element–binding protein (SREBP1c), a master regulator transcription factor that induces lipogenic genes expression (5). This elevates hepatic lipid production and redistribution to white adipose tissue (WAT) for storage, causing visceral obesity. With persistent nutritional burden, insulin resistance develops in WAT, manifested by lipolysis and progression of a proinflammatory state (6).

Released fatty acids from WAT could redistribute to other tissues, in particular the liver (the portal hypothesis), causing lipotoxicity and insulin resistance (7,8). Increased fatty acid supply causes insulin resistance (9) by impairing insulin clearance through protein kinase C-δ–mediated mechanisms (10) and contributing to lipid accumulation in hepatocytes, which, in turn, induces a local inflammatory response (11). In addition, the rise in WAT-derived adipokines modulates the intrahepatic proinflammatory milieu to contribute to pathways amplifying insulin resistance (6). Thus, systemic inflammation in diet-induced obesity occurs late in the progression of the disease (12) by

[1]Center for Diabetes and Endocrine Research, College of Medicine and Life Sciences, The University of Toledo, Toledo, OH
[2]Department of Physiology and Pharmacology, College of Medicine and Life Sciences, The University of Toledo, Toledo, OH
[3]Department of Rehabilitation Sciences, College of Health Sciences, The University of Toledo, Toledo, OH
[4]Program in Molecular Medicine, University of Massachusetts Medical School, Worcester, MA
[5]Research Division, Joslin Diabetes Center, Harvard Medical School, Boston, MA
[6]Section of Endocrinology and Metabolism, Department of Internal Medicine, Yale University School of Medicine, New Haven, CT

Corresponding author: Sonia M. Najjar, sonia.najjar@utoledo.edu.

Received 18 November 2014 and accepted 16 March 2015.

This article contains Supplementary Data online at http://diabetes.diabetesjournals.org/lookup/suppl/doi:10.2337/db14-1772/-/DC1.

Q.Y.A.-S., A.M.D., and S.G.L. contributed equally to this work.

comparison with hyperinsulinemia and insulin resistance (13,14).

In addition to increased insulin secretion, impaired insulin clearance contributes to mounting hyperinsulinemia in obese humans (15,16) and dogs (17) and in subjects at high risk for metabolic syndrome (18) and type 2 diabetes (19). Furthermore, studies demonstrate that an ~10% weight loss improves insulin clearance (20) but not secretion, which requires a more significant weight loss (16). Consistent with a role for the carcinoembryonic antigen-related cell adhesion molecule 1 (CEACAM1) in promoting receptor-mediated insulin uptake and degradation in hepatocytes (21), hepatic insulin clearance is impaired in mice with liver-specific CEACAM1 inactivation (L-SACC1) or global mutation ($Cc1^{-/-}$) (22–24). This is followed by hyperinsulinemia and insulin resistance (22–24) in addition to elevated lipid production in liver and accumulation in WAT (25). Hyperinsulinemia in $Cc1^{-/-}$ mice occurs without altered insulin secretion despite loss of CEACAM1 from β-cells (23). Thus, studies on CEACAM1 provide convincing evidence that hyperinsulinemia resulting from impaired insulin clearance causes insulin resistance and visceral obesity.

Moreover, hepatic CEACAM1 levels are markedly reduced in humans with insulin resistance, obesity, and fatty liver disease (26). Because dietary factors play an important role in the development of insulin resistance, we investigated whether administration of a high-fat (HF) diet represses CEACAM1-dependent insulin clearance pathways in C57/BL6J mice (BL6) and whether this plays a role in diet-induced insulin resistance.

RESEARCH DESIGN AND METHODS

Mice Generation

Transgenic mice with liver-specific overexpression of rat CEACAM1 (L-CC1) were generated using human apolipoprotein A1 (APOA1) promoter/enhancer element (27) (Fig. 1*A*), as described (22). The "minigene" construct was obtained by subcloning 519 nucleotides of proximal APOA1 promoter 5′ of a *Ceacam1* rat minigene containing intron1. This was subcloned into plasmid cytomegalovirus (pCMV)-3Tag-3A plasmid at *Not1* site to encode a FLAG-tagged rat CEACAM1 protein. The 3′-FLAG-tagged APOA1/wild-type (WT) rat *Ceacam1* minigene was excised and injected in the pronuclei of single-cell fertilized mouse embryos from SJLXC57Bl/6J matings (Yale Transgenic Facility). PCR analysis of tail genomic DNA was used to identify 11 F_0 founders. Two lines were identified and backcrossed six times on the BL6 background (The Jackson Laboratory).

Mice were kept in a 12-h dark/light cycle. Male mice (2 months old) were fed ad libitum a standard regular diet (RD) deriving 12% calories from fat, 66% from carbohydrate, and 22% calories from protein or a high-calorie HF diet deriving 45% of calories from fat, 35% from carbohydrate, and 20% from protein (Catalog #D12451, Research Diets). Fatty acid composition in the HF diet was 36% saturated fatty acids, 45% monounsaturated fatty acids, and 19% polyunsaturated fatty acids. The Institutional Animal Care and Utilization Committee approved all procedures.

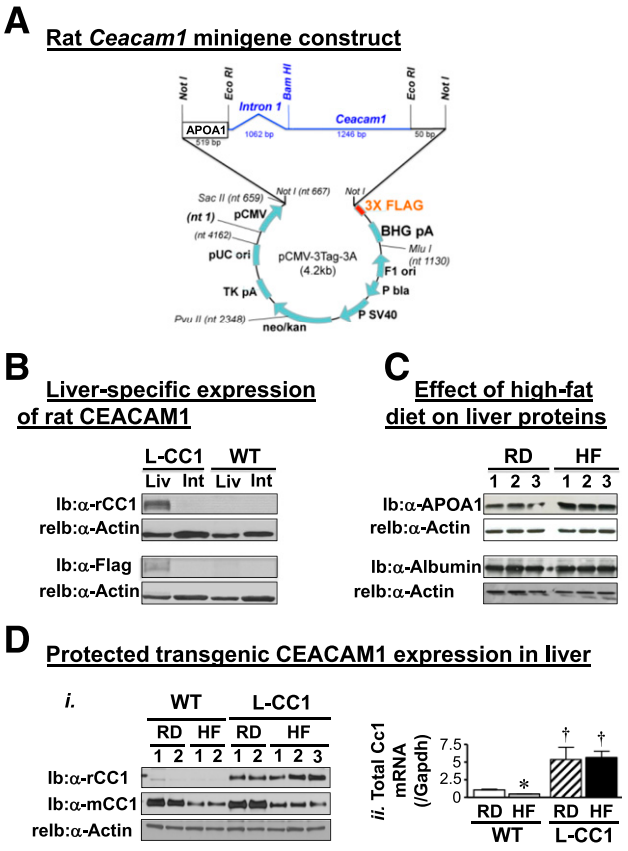

Figure 1—Generation of L-CC1 transgenic mice with liver-specific overexpression of CEACAM1. *A*: L-CC1 transgenic mice overexpressing FLAG-tagged WT rat CEACAM1 in the liver were generated using the human APOA1 promoter/enhancer element. The "minigene" construct was obtained by subcloning 519 nucleotides of proximal APOA1 promoter 5′ of a *Ceacam1* rat minigene containing intron 1, subcloned into plasmid cytomegalovirus (pCMV)-3Tag-3A plasmid at *Not1* site to encode a FLAG-tagged rat CEACAM1 protein. *B*: Liver (Liv) and intestinal (Int) lysates were analyzed by immunoblotting (Ib) with polyclonal antibodies against rat CEACAM1 (α-rCC1) and FLAG (α-FLAG), followed by reprobing (relb) with α-actin antibody for protein normalization. Gels represent more than two experiments on more than three mice per genotype. *C*: Western analysis of liver proteins from WT mice fed the RD or HF diet for 30 days with α-APOA1 and albumin polyclonal antibodies (n = 3 per group). Data indicate induced expression of APOA1, but not albumin, by the HF diet. Gels represent more than two experiments on two different sets of mice. *Di*: WT and L-CC1 mice were fed the HF or RD for 4 months before liver lysates were analyzed by Western blotting using antibodies against rat (rCC1) and mouse (mCC1) proteins, followed by α-actin for normalization. *Dii*: Liver lysates were also analyzed by quantitative RT-PCR to determine mRNA of Ceacam1 using primers common to both rat and mouse genes (total Ceacam1) and normalized to GAPDH. *P < 0.05 HF vs. RD per genotype. †P < 0.05 L-CC1 vs. WT per same feeding group.

Metabolic Parameters

Retro-orbital venous blood was drawn at 1100 h from mice fasted overnight to assess plasma insulin levels (Linco

Research), nonesterified fatty acids (NEFA C; Wako), triacylglycerol (Pointe Scientific), and fibroblast growth factor 21 (FGF21; BioVendor) (23).

Body Composition

Whole-body composition was assessed by ^{1}H-MRS (Echo Medical Systems).

Hyperinsulinemic-Euglycemic Clamp Analysis

A 2-h hyperinsulinemic-euglycemic clamp was performed in awake overnight-fasted mice (n = 10 per feeding group per genotype) with primed and continuous infusion of human regular insulin (Humulin) at a rate of 2.5 mU $\cdot$ kg^{-1} $\cdot$ min^{-1} (23). Glucose metabolism was estimated with a continuous infusion of 0.05 μCi/min of [3-^{3}H]glucose (PerkinElmer and Analytical Sciences) before and 0.1 μCi/min throughout the clamp. Insulin levels were measured using the Mouse Ultrasensitive Insulin ELISA Kit from Alpco.

Glucose and Insulin Tolerance Tests

Awake overnight-fasted mice were injected intraperitoneally (i.p.) with 1.5 g/kg body weight (BW) dextrose solution before glucose was measured in tail blood. For insulin tolerance, mice were fasted for 6 h, injected with human regular insulin (Novo Nordisk; 0.75 units/kg BW i.p.), and their glucose was measured.

In Vivo Insulin Clearance

Human [^{125}I]insulin (1640Bq/mouse; PerkinElmer) was injected in overnight-fasted anesthetized mice via tail vein, and retro-orbital blood was immediately drawn every 10 s for 2 min (22,24). Blood radioactivity was counted (gamma-counter), and the insulin clearance rate was calculated as the percentage of 10-s postintravenous radioactivity.

Glucose Uptake in Muscle

Glucose uptake in response to insulin (1,200 pmol/L) was measured in soleus muscle from hind limbs of fasted mice in the presence of 2-deoxy-D-[l,2-^{3}H]glucose (DG, 1 mmol/L) and [U-^{14}C]mannitol (39 mmol/L) (22). Muscle was frozen in liquid nitrogen, and the intracellular 2-DG level was measured in nmol $\cdot$ g wet muscle^{-1} $\cdot$ min^{-1}.

Ex Vivo Palmitate Oxidation

Soleus and gastrocnemius muscle of overnight-fasted mice were assayed as described (28) with modifications (29). Muscle was homogenized in 10 mmol/L Tris (pH 7.2), 300 mmol/L sucrose, and 2 mmol/L EDTA, injected by syringe into a sealed beaker to be incubated at 30°C for 45 min in the presence of 0.2 mmol/L of [1-^{14}C]palmitate (0.5 μCi/mL) and 2 mmol/L ATP in incubation buffer (100 mmol/L sucrose, 10 mmol/L Tris-HCl, 5 mmol/L potassium phosphate, 80 mmol/L KCl, 1 mmol/L $MgCl_2$, 2 mmol/L L-carnitine, 0.1 mmol/L malic acid, 0.05 mmol/L CoA, 1 mmol/L dithiothreitol, 0.2 mmol/L EDTA, and 0.5% BSA, pH 7.4). The reaction was terminated with glacial acetic acid, and trapped CO_2 radioactivity was measured by liquid scintillation in CytoScint (MP Biomedicals).

Primary Hepatocytes

Hepatocytes were isolated by perfusing liver (1 mL/min) with collagenase type II solution (1 mg/mL) (Worthington) (22). Cells were dispensed in Williams E complete media (10 mmol/L lactate, 10 nmol/L dexamethasone, 100 nmol/L insulin, 10% FBS, and 1% penicillin-streptomycin), counted, and plated onto 12-well cell culture plates at 2.5 $\times$ 10^{5}/well density and incubated at 37°C for 48 h. Cells from HF-fed mice were supplemented with 0.1 mmol/L fatty acid (0.035 mmol/L palmitic acid, 0.045 mmol/L oleic acid, and 0.02 mmol/L linoleic acid, and 2 mmol/L insulin-free BSA [Sigma-Aldrich A7888] at a 1:5 ratio). Medium was changed 24 h after plating.

Primary Proximal Tubule Cells

Kidney cortices were finely cut, reconstituted in 1 mL Solution 1 (DMEM-F12, 1 mmol/L heptanoate acid and 4 mmol/L glycine, pH 7.4), digested three times (shaking at 37°C in 100% oxygen for 12 min) in 10 mL collagenase solution (1 mg/mL collagenase type II [Worthington], 1 mg/mL insulin-free BSA, and 0.1 mg/mL DNase I [Sigma-Aldrich]), and allowed to settle down into a sterile pipette (30). Supernatant was centrifuged at 1,000 rpm at 4°C for 5 min, and the cell pellet was reconstituted in Percoll Solution (colloidal silica particles of 15–30 nm diameter, 23% w/w in water, coated with polyvinyl-pyrrolidone [Sigma-Aldrich]), and ultracentrifuged (17,000 rpm at 40°C for 30 min). Cells between the third and fourth layer at ~1.0–1.3 g/mL Percoll density were collected, washed twice in 50 mL Solution 1 (1,000 rpm, 4°C, 5 min), and incubated in six-well plates for 3–5 days in DMEM/F-12 culture medium (Sigma-Aldrich), containing 1% penicillin-streptomycin, 60 nmol/L sodium selenite, 1.1 mg/mL sodium bicarbonate, 5 μg/mL human apo-transferrin, 2 mmol/L glutamine, 50 nmol/L dexamethasone, 5 pmol/L 3,5,3′-triiodothyronine, 25 ng/mL prostaglandin E1, 50 nmol/L hydrocortisone, 10 ng/mL epidermal growth factor, 5 μg/mL insulin, 3.1 g/L D-glucose, 2% (vol/vol) FBS, and 20 mmol/L HEPES, pH 7.4 (Invitrogen and Sigma-Aldrich). The fatty acid mixture (above) containing 10 mmol/L lactate was added to cells from HF-fed mice. Medium was changed 24 h after plating. Cells were kept in the culture medium for 48–72 h.

Ligand Binding and Internalization in Cells

[^{125}I]insulin (Human [^{125}I]-insulin, PerkinElmer) (30,000 cpm) was allowed to bind to isolated cells at 4°C for 5 h in cold Krebs-Ringer phosphate buffer (100 mmol/L HEPES, pH 7.4; 120 mmol/L NaCl, 1.2 mmol/L $MgSO_4$, 1 mmol/L EDTA, 15 mmol/L CH_3COONa, 10 mmol/L glucose, and 1% BSA). Unbound insulin was removed in cold 1 $\times$ PBS, and cells were incubated in 1 mL Krebs-Ringer phosphate buffer at 37°C for 0–90 min, washed, and incubated with 900 μL acidic PBS (pH 3.5) for 10 min on ice to remove surface-bound insulin. Hepatocytes were washed and lysed with 0.4N NaOH to account for cell-associated internalized insulin. The acid wash was counted as surface-bound and NaOH-solubilized cells as internalized cell-associated ligand. Internalized insulin was calculated as percent

cell-associated per specifically bound ligand (the sum of surface-bound plus cell-associated ligand).

β-Cell Area and Immunohistochemistry

Pancreas was weighed, fixed in Bouin solution, sectioned, and stained (23). Antibodies were guinea pig anti-human insulin (Linco Research) and aminomethylcourmain -conjugated donkey anti-guinea pig antibody (Jackson ImmunoResearch) for insulin and anti-mouse glucagon monoclonal antibody (Sigma-Aldrich) and Texas red-conjugated donkey anti-mouse antibody (Jackson ImmunoResearch) for glucagon. Areas of β-cells and α-cells were calculated by morphometric analysis using ImageJ software (National Institutes of Health; http://rsb.info.nih.gov/ij/) and divided by total pancreas area.

Western Analysis

Proteins were analyzed by 7% SDS-PAGE and immunoprobing with polyclonal antibodies against phospho-Akt (Ser^{473}, Cell Signaling Technology), followed by α-Akt antibody. Also used were polyclonal antibodies against mouse CEACAM1 (25), rat CEACAM1 (α-rCC1) (23), and fatty acid synthase (α-Fasn) (25). For normalization, monoclonal antibodies against actin, GAPDH, and tubulin (Sigma-Aldrich or Santa Cruz Biotechnology) were used. Blots were incubated with horseradish peroxidase-conjugated anti-goat IgG (Santa Cruz Biotechnology), anti-mouse or anti-rabbit IgG (Amersham) antibodies, subjected to enhanced chemiluminescence (Amersham), and quantified by densitometry (ImageJ software).

Northern Analysis

mRNA was purified using TRIzol (Invitrogen), followed by the MicroPoly(A) Pure kit (Ambion) and analysis by probing with Ceacam1 cDNAs, using the Random Primed DNA Labeling Kit (Roche), before reprobing and normalizing to β-actin.

Semiquantitative Real-Time RT-PCR

Total RNA was isolated with PerfectPure RNA Tissue Kit (5 Prime) following the manufacturer's protocol. cDNA was synthesized by ImProm-II Reverse Transcription System (Promega), using 1 μg total RNA and oligo dT primers (Supplementary Table 1). cDNA was evaluated with quantitative RT-PCR (StepOnePlus, Applied Biosystems). mRNA was normalized to GAPDH or 18S.

Statistical Analysis

Data were analyzed with SPSS software by two-way ANOVA or the two-tailed Student *t* test with GraphPad Prism 4 software. $P < 0.05$ was statistically significant.

RESULTS

HF Diet Causes Insulin Resistance

HF feeding for 9–30 days progressively increased visceral obesity and, subsequently, lipolysis and plasma NEFA in WT mice (Table 1). In parallel, it caused insulin resistance, manifested by fed hyperglycemia (Table 1) and glucose and insulin intolerance beginning at 21 days (Fig. 2*A*, *i* and *ii*, respectively). Given that overnight fasting reverses diet-induced glucose intolerance, particularly in liver (31), it is possible that hepatic insulin resistance may have occurred earlier. Nonetheless, Western analysis revealed that an insulin surge after 7 h of refeeding (25) (358. ± 47.8 vs. 39.1 ± 3.16 pmol/L at fasting; $P < 0.05$) induced Akt phosphorylation (by ~2- to 10-fold) in liver, soleus muscle, and WAT of mice fed an RD (Supplementary Fig. 1*A*, *i*). In mice fed an HF diet for 28 days, however, insulin release after refeeding (1,128. ± 70.53 vs. 38.72 ± 1.408 pmol/L at fasting; $P < 0.05$) induced Akt phosphorylation in muscle and WAT, but not liver. Together, this shows altered insulin signaling in liver by HF.

HF Diet Impairs Insulin Clearance and Causes Hyperinsulinemia

HF feeding for 30 days caused hyperinsulinemia (Table 1) that could result partly from the compensatory increase in insulin secretion, as demonstrated by the more robust acute-phase insulin release in response to the intraperitoneal injection of glucose (data not shown).

Table 1—Effect of HF diet on plasma and tissue biochemistry in BL6 male mice

	9 days		30 days	
	RD	HF	RD	HF
Visceral fat/body weight (%)	1.2 ± 0.1	1.9 ± 0.1*	1.4 ± 0.3	3.8 ± 0.4*
Fasting plasma				
NEFA (mEq/L)	0.5 ± 0.1	0.7 ± 0.1	0.5 ± 0.1	1.0 ± 0.1*
Insulin (pmol/L)	36.2 ± 0.72	39.9 ± 1.04	35.6 ± 1.66	59.8 ± 5.84*
C-peptide (pmol/L)	266. ± 34.0	277. ± 22.0	307. ± 53.2	351. ± 39.8
C-peptide–to–insulin molar ratio	8.0 ± 0.2	7.0 ± 0.1	9.0 ± 0.1	5.1 ± 0.0*
Hepatic triacylglycerol (μg/mg protein)	183. ± 23.8	312. ± 67.6	166. ± 21.1	688. ± 128.*
Blood glucose (mg/dL)				
Fasting	100. ± 2.10	104. ± 5.60	96.5 ± 5.90	111. ± 7.00
Fed	101. ± 5.31	108. ± 7.02	103. ± 4.41	136. ± 14.9*

Mice (4 months of age, $n > 6$ per feeding group) were fed RD or HF for 9 or 30 days. Values are expressed as mean ± SEM. *$P < 0.05$ HF vs. RD per feeding period.

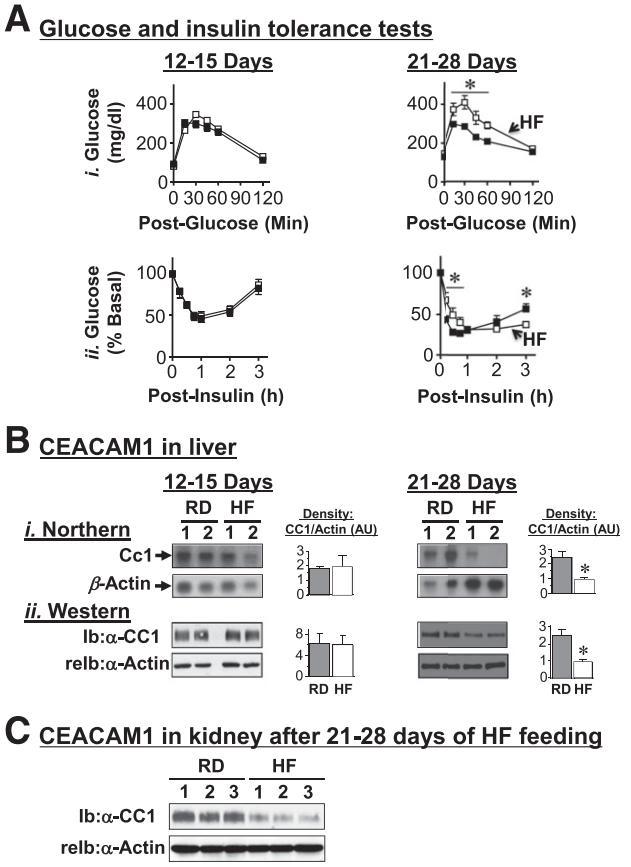

Figure 2—Effect of HF diet on insulin and glucose tolerance and on CEACAM1 protein levels. *A*: BL6 mice (2 months old) were fed an RD (■) or an HF diet (□) for 12–28 days before they were challenged with an intraperitoneal injection of glucose (1.5 g/kg BW) *(i)* or insulin (0.75 units/kg body weight) *(ii)* to assess blood glucose levels at 0–180 min postinjection. **P* < 0.05 HF vs. RD (*n* > 6 per feeding group). *B*: Liver lysates were subjected to Northern *(i)* and Western *(ii)* analyses and reprobing with β-actin cDNA and α-actin antibody, respectively, for normalization (*n* > 6 mice per feeding group). Bands were scanned, and the density was measured with arbitrary units (AU) and represented in the right-hand graphs. The numbers above the gel denote different mice. **P* < 0.05 vs. RD. *C*: Kidney lysates from three mice per feeding group were subjected to sequential Ib with α-mouse CEACAM1 antibody, followed by reprobing (relb) with α-actin antibody for normalization.

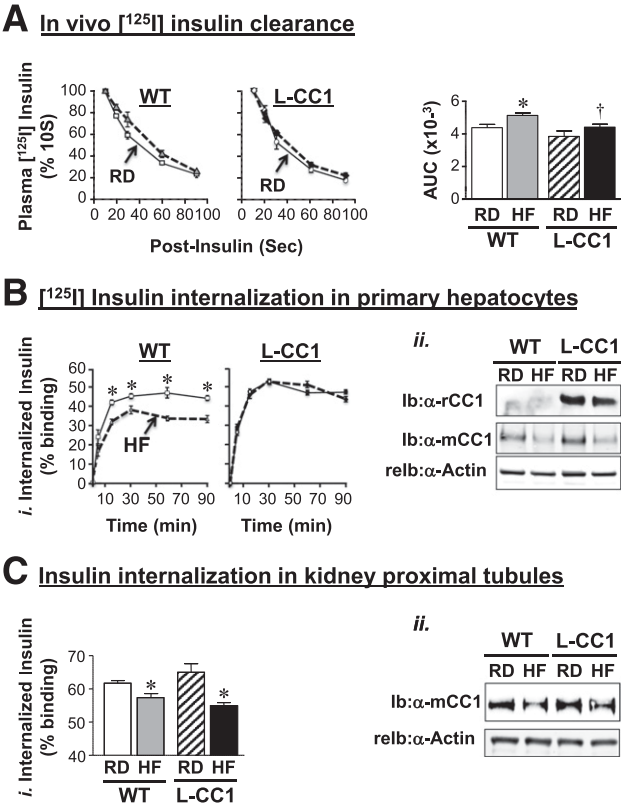

Figure 3—Effect of HF diet on insulin clearance. *A*: Metabolic clearance of ^{125}I-insulin injected in the tail vein was measured in 4-month-old mice (*n* = 8 mice per feeding group per genotype) fed the HF diet (dashed lines) or the RD (solid lines) for 1 month. Blood ^{125}I-insulin was counted after 10–90 s postinjection. Values are expressed as mean ± SEM of percent of the amount of blood insulin at 10 s. AUC of the decrease in plasma insulin with postinjection time was calculated and is presented in the accompanying bar graph. *Bi*: ^{125}I-insulin internalization in primary hepatocytes derived from mice fed an HF (dashed lines) or RD (solid lines) for 4 months was measured. After binding, ^{125}I-insulin was allowed to internalize at 37°C for 0–90 min (horizontal axis). Internalized ligand was plotted on the vertical axis as percent of the specifically bound ligand. Values are expressed as mean ± SD from triplicate experiments performed on more than three mice per feeding group per genotype. *Bii*: Western blot analysis of lysates of primary hepatocytes to analyze the amount of rat (rCC1) and mouse (mCC1) CEACAM1 normalized to actin. *Ci*: Primary proximal tubule cells were isolated from at least eight mice per feeding group per genotype, mixed, and subjected to ^{125}I-insulin internalization. The experiment was repeated three times. *Cii*: Some aliquots of isolated cells were lysed and analyzed by Western blot to assess CEACAM1 level normalized to actin. A representative gel of more than two experiments is shown. *A–C*: Values are expressed as mean ± SEM. **P* < 0.05 HF vs. RD per genotype. †*P* < 0.05 L-CC1 vs. WT per same feeding group.

Diet-induced hyperinsulinemia could also result from impaired hepatic insulin clearance, as supported by *a*) the significant approximately twofold decrease in steady-state C-peptide–to–insulin molar ratio by HF intake for 30, but not 9 days (Table 1), and *b*) the higher amount of residual ^{125}I-labeled plasma insulin within 90 s after an intravenous injection in HF-fed relative to RD-fed WT mice as measured by the area under the curve (AUC) of the decrease in plasma insulin with postinjection time (Fig. 3*A*, accompanying graph). That injected insulin is cleared less efficiently could explain the sustained decrease in glucose levels in HF-treated mice in some experiments (Fig. 2*A*, *ii*, right panel).

We then examined the effect of HF on CEACAM1 expression. Northern and Western analyses showed a decline in CEACAM1 mRNA and protein levels by >50% after 21–28 days of HF feeding in the liver (Fig. 2*B*) and kidney (Fig. 2*C*), the two main sites of insulin clearance.

Role of Hepatic CEACAM1 Overexpression in Diet-Induced Insulin Resistance

Because CEACAM1 mediates insulin clearance, we then investigated whether the observed decrease of CEACAM1

in response to HF contributed mechanistically to hyperinsulinemia-driven insulin resistance. To this end, we generated transgenic mice (L-CC1) overexpressing FLAG-tagged rat CEACAM1 in the liver, using a human APOA1 promoter (22) (Fig. 1*A*). Immunoblotting (Ib) with α-Flag and α-rat CEACAM1 (α-rCC1) antibodies demonstrated expression of the WT rat transgene in the liver (Fig. 1*B*, Liv) but not intestine (Fig. 1*B*, Int), the other main site of APOA1 production (32), as was the case for L-SACC1 mice (22). Unlike endogenous mouse CEACAM1, which underwent a >50% reduction (Fig. 1*D*, *i*; Ib: α-mCC1), transgenic rat CEACAM1 protein was protected (Ib: α-rCC1) even after 4 months of HF intake. Quantitative RT-PCR analysis using primers that bind to mouse and rat Ceacam1 showed that HF failed to lower total Ceacam1 mRNA levels (Fig. 1*D*, *ii*), likely owing to APOA1 induction by the HF diet (Fig. 1*C*).

As opposed to WT mice, HF did not significantly alter the AUC of plasma residual ^{125}I-insulin 90 s after tail vein injection in L-CC1 mice, keeping it at a comparable level to that in RD-fed WT mice (Fig. 3*A*, accompanying graph). Consistently, ^{125}I-insulin internalization was markedly lower in hepatocytes isolated from WT mice fed HF for 4 months, but not L-CC1 mice (Fig. 3*B*, *i*) in parallel to preserved CEACAM1 protein levels in transgenic mice (Fig. 3*B*, *ii*). As a control, we analyzed insulin internalization in kidney cells, which express CEACAM1 and contribute to a lower degree to insulin clearance (33). HF reduced ^{125}I-insulin internalization in primary proximal tubule cells from both mouse groups (Fig. 3*C*, *i*), consistent with reduction of their CEACAM1 protein levels (Fig. 3*C*, *ii*). In parallel, HF did not alter plasma insulin levels in L-CC1 after 30 days (Supplementary Table 2) and only slightly (by ~1.3-fold) induced it after 4 months, as opposed to WT mice in which it elevated insulin levels by ~2- to 2.5-fold after 1–4 months (Tables 1 and 2). The data are consistent with protected hepatic, but not renal insulin clearance in L-CC1 mice, an event that limits HF-induced hyperinsulinemia.

HF intake for 28 days did not alter Akt activation in L-CC1 liver in response to the fourfold rise in insulin upon refeeding (Supplementary Fig. 1*A*, *ii*), nor did it affect glucose or insulin tolerance (Supplementary Fig. 1*B*). To assess the effect of prolonged HF intake in vivo, a 2-h hyperinsulinemic-euglycemic clamp was performed on mice fed HF for 4 months (Fig. 4*A*). Basal glucose at the beginning of the clamp (not shown) and basal hepatic glucose production (Fig. 4*A*, *i*), a measure of rate of appearance at the preclamp condition, were similar in both groups of mice fed RD or HF. During the clamp, at comparable glucose (Fig. 4*A*, *ii*) and insulin (Fig. 4*A*, *iii*) levels, HF reduced the glucose infusion rate required to maintain euglycemia in L-CC1 mice to a much lesser extent than in WT mice, leading to an approximately twofold higher glucose infusion rate in HF-fed transgenic mice (Fig. 4*A*, *iv*). Consistently, HF reduced the ability of insulin to suppress hepatic glucose production (by ~45%) and whole-body glucose disposal in WT but not L-CC1 mice (Fig. 4*A*, *v* and *vi*, respectively). Moreover, HF induced whole-body glycolysis in L-CC1 mice (Fig. 4*A*, *vii*), contributing to higher glucose turnover compared with HF-fed WT mice. In contrast, glycogen synthesis was comparable in WT and L-CC1 mice under both feeding conditions (not shown). Contributing to higher glucose turnover in HF-fed L-CC1 mice and a higher glucose infusion rate during the hyperinsulinemic-euglycemic clamp was the rise of glucose uptake in response to submaximal concentrations of insulin (0.3 mU/mL) in the oxidative soleus muscle of HF-fed transgenic mice (Fig. 4*B*). That systemic insulin sensitivity is preserved is also supported by the limited induction of lipolysis (assessed by fasting plasma NEFA levels) after 1–4 months of HF feeding in L-CC1 mice, by comparison with WT mice, where HF-induced lipolysis was observed (Table 2 and Supplementary Table 2). Taken together, the data suggest that liver-specific CEACAM1 overexpression restricted the adverse effect of a sustained HF diet on insulin action.

Consistent with the well-known increase in insulin secretion to compensate for insulin resistance, HF feeding

Table 2—Effect of HF diet for 4 months on plasma and tissue biochemistry

	WT		L-CC1	
	RD	HF	RD	HF
Body weight (g)	25. ± 1.0	35. ± 2.0*	25. ± 0.1	32. ± 1.0*
Total fat mass (g)	1.8 ± 0.3	13. ± 1.1*	2.1 ± 0.3	9.6 ± 0.8*†
Total lean mass (g)	24.3 ± 0.42	25.4 ± 0.41	24.6 ± 0.44	24.9 ± 0.53
Fasting plasma				
C-peptide–to–insulin molar ratio	12.1 ± 0.68	8.62 ± 0.31*	11.2 ± 0.62	11.1 ± 0.52†
Insulin (pmol/L)	68.1 ± 3.54	153. ± 15.2*	60.4 ± 4.25	87.6 ± 6.72*†
NEFA (mEq/L)	0.60 ± 0.02	0.86 ± 0.04*	0.62 ± 0.03	0.70 ± 0.04†
Hepatic triacylglycerol (μg/mg protein)	131. ± 5.80	450. ± 15.0*	140. ± 8.30	160. ± 11.1†
Fed blood glucose (mg/dL)	133. ± 2.20	162. ± 3.45*	132. ± 4.10	142. ± 3.68†

Mice (n >10/feeding group/genotype) were fed an HF diet for 4 months starting at 2 months of age. Lean mass (g) and fat mass (g) were determined using MRS. Values are expressed as mean ± SEM. *P < 0.05 HF vs. RD per genotype. †P < 0.05 L-CC1 vs. WT per feeding group.

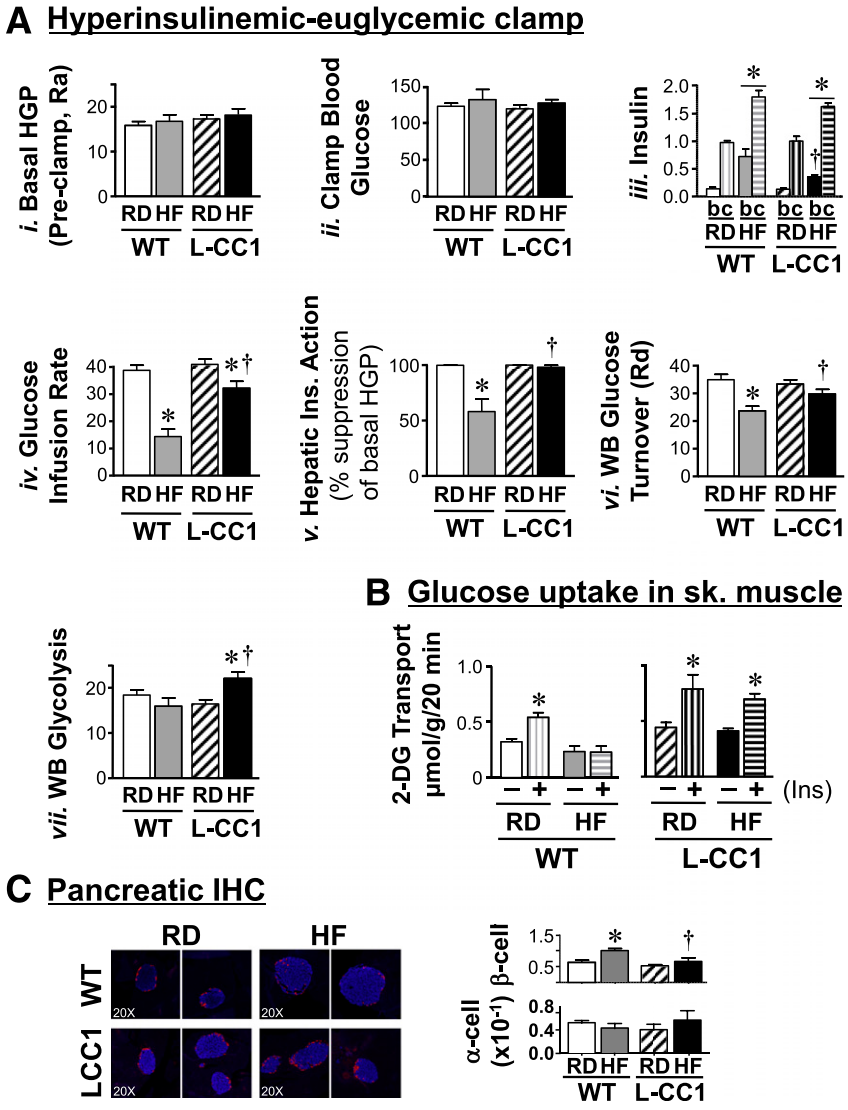

Figure 4— Insulin action in response to prolonged HF diet. *A*: Overnight-fasted, awake 6-month-old mice fed the RD or HF diet for 4 months ($n \geq 8$ per feeding group per genotype) were subjected to a 2-h hyperinsulinemic-euglycemic clamp. Values are expressed as mean ± SEM in mg/dL for hepatic glucose production (HGP) levels (Ra, rate of appearance), in ng/mL for insulin, and in mg/min/kg for all other measurements. Rd, rate of disposal. *$P < 0.05$ HF vs. RD per genotype. †$P < 0.05$ L-CC1 vs. WT per feeding group. All clamp (c) insulin values were significantly higher than basal (b) per the same mouse group regardless of the diet, but for simplicity, the symbol is not shown. *B*: Uptake of 2-deoxyglucose (2-DG) in the absence (−) or presence (+) of insulin was measured in soleus muscle isolated from mice fed an HF diet for 6 months. Values are expressed as mean ± SEM. *$P < 0.05$ vs. no insulin. *C*: Pancreas sections from mice fed an HF diet for 4 months were fixed and immunostained with antibodies against insulin (blue) and glucagon (red). β-Cell and α-cell areas were estimated by morphometric analysis of 30–40 islets from each mouse group. Values are expressed as mean ± SEM in arbitrary units and presented in the graph. Photomicrographs are shown at original magnification ×20. *$P < 0.05$ HF diet vs. RD per genotype. †$P < 0.05$ L-CC1 vs. WT per feeding group.

for 4 months caused an increase in β-cell area of WT but not L-CC1 mice, as assessed by immunohistochemical analysis with α-insulin antibody (blue) (Fig. 4*C*). Immunostaining with α-glucagon antibody (red) revealed failure of HF feeding to alter α-cell area in WT and L-CC1 mice (Fig. 4*C*, graph).

Role of Hepatic CEACAM1 Overexpression in Diet-Mediated Alteration of Hepatic Lipid Metabolism

HF feeding for 30 days significantly induced hepatic mRNA levels of *Srebp1c* in WT (1.93 ± 0.25 vs. 0.93 ± 0.07; $P <$ 0.05), but not L-CC1 mice (1.23 ± 0.10 vs. 0.90 ± 0.15). Consistently, the protein level of Fasn, a transcriptional target of Srebp1c, was induced by HF in WT, but not L-CC1 mice (Fig. 5*A*). This could contribute to mechanisms underlying increased triacylglycerol content in the liver of HF-fed WT mice (Tables 1 and 2 and Supplementary Table 2).

Lower lipid accumulation in L-CC1 livers could relate partly to elevated fatty acid β-oxidation under both feeding conditions (Fig. 5*B*, *i*). The parallel higher levels of plasma FGF21 in L-CC1 versus WT mice under both feeding

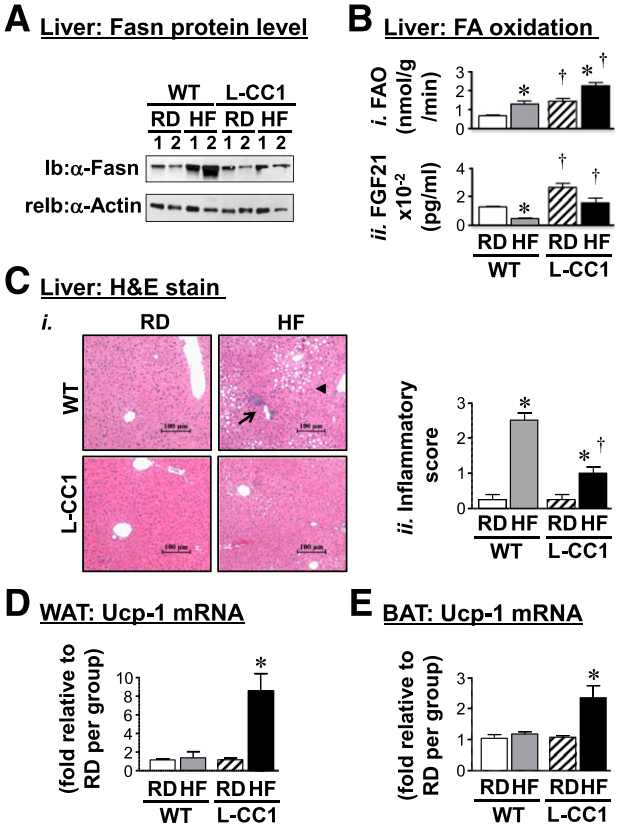

Figure 5—Effect of prolonged HF diet on lipid metabolism in liver. *A*: Liver lysates were subjected to Western analysis with α-Fasn, followed by α-actin antibody for normalization. Gel represents two mice per each feeding group. Experiments were repeated twice. *B*: Hepatic FAO (*i*) and plasma FGF21 (*ii*) levels were determined in mice fed the RD or HF diet per mouse group ($n > 6$ per feeding group per genotype). Experiments were repeated at least three times. Values are expressed as mean ± SEM. *$P < 0.05$ HF vs. RD per genotype. †$P < 0.05$ L-CC1 vs. WT per feeding group. *Ci*: Liver histology was assessed in hematoxylin and eosin stained sections ($n > 4$ mice per feeding group per genotype). In WT, HF feeding caused predominantly microvesicular lipid infiltration (arrowhead) alternating with normal liver parenchyma. It also caused portal mononuclear inflammatory cell foci (arrow) in WT but not in L-CC1 mice, in which neither lipid nor inflammatory infiltration was almost absent. Representative images from three sections per mouse are shown. *Cii*: Inflammatory islands from mice were counted in four sections per mouse, scored on a scale of 0–3, and plotted. Values are expressed as mean ± SEM. *$P < 0.05$ HF vs. RD per genotype. †$P < 0.05$ L-CC1 vs. WT per feeding group. WAT (*D*) and BAT (*E*) were lysed and mRNA levels analyzed in duplicates ($n > 5$ mice per feeding group per genotype). Values are expressed as mean ± SEM. *$P < 0.05$ HF vs. RD per genotype.

conditions (Fig. 5*B*, *ii*) could explain this finding because it reflects primarily hepatic FGF21 levels (34).

Histological evaluation of hematoxylin and eosin–stained liver sections of mice fed HF for 4 months revealed diffused fat infiltration with predominantly microvesicular steatosis and a mix of macrosteatosis in livers from HF-fed WT mice (Fig. 5*C*). In contrast, HF-fed L-CC1 mice showed more fat-free parenchyma with small affected areas.

Moreover, HF-fed WT livers exhibited more inflammatory foci than HF-fed L-CC1 (Fig. 5*C*), as supported by the 10-fold induction by HF in WT versus 4-fold in L-CC1 (Fig. 5*C*, *ii* graph). Consistently, HF caused a twofold increase in CD68 mRNA in WT but not L-CC1 (Supplementary Fig. 2). Because CD68 is an antigen expressed in macrophages manifesting phagocytosis (35), the data support a lower inflammatory state in HF-fed L-CC1 than in WT mice.

Role of Hepatic CEACAM1 Overexpression in Diet-Mediated Alteration of Energy Balance

Consistent with induction of brown adipogenesis by FGF21 (36,37), mRNA levels of Ucp1, a key gene in brown adipogenesis, were elevated in WAT and brown adipose tissue (BAT) of L-CC1 but not WT after 4 months of HF intake (Fig. 5*D* and *E*, respectively).

This prompted us to assess energy expenditure in these mice. Daily food intake of L-CC1 was similar to that in WT mice when fed RD or HF for 4 months (Fig. 6*A*). Indirect calorimetry analysis over a 24-h period revealed comparable energy expenditure (heat generation) (Fig. 6*B*), VO_2 (Fig. 6*B*), VCO_2 (Fig. 6*C*), and spontaneous locomotor activity (Fig. 6*D*) in L-CC1 and WT mice under normal feeding conditions. Owing to normal VO_2 and VCO_2 levels, the respiratory exchange ratio was also normal in L-CC1 mice (0.899 ± 0.004) versus WT (0.875 ± 0.008). HF feeding markedly reduced energy expenditure and VO_2 in WT but not in L-CC1 mice (Fig. 6*B*), in addition to causing a slight reduction in VCO_2 in L-CC1 mice (Fig. 6*C*). The respiratory exchange ratio was reduced to a similar extent in both groups of mice upon HF feeding (0.801 ± 0.008 in HF-fed L-CC1 and 0.780 ± 0.013 in HF-WT mice). Moreover, HF caused a marked reduction in spontaneous locomotor activity of WT but not L-CC1 mice (Fig. 6*D*). Preserved energy expenditure and physical activity could contribute to lower fat mass in HF-fed L-CC1 than in HF-fed WT mice (Table 2).

DISCUSSION

The notion that hyperinsulinemia causes insulin resistance has gained traction from observations in clinical studies (1–3) as well as from our studies on *Ceacam1* mutant mice (22–24). Moreover, reduced insulin clearance, which could cause hyperinsulinemia, has emerged as a risk factor for metabolic syndrome (18) as well as type 2 diabetes, in particular among Hispanics and African Americans (19). Because hepatic CEACAM1 content is reduced in patients with obesity, insulin resistance, and fatty liver disease (26), the current studies addressed the role of altered CEACAM1-dependent insulin clearance in hyperinsulinemia and insulin resistance in response to HF, a global health risk factor. We show that HF reduced hepatic CEACAM1 levels by >50% within 21 days in WT mice. Consistent with the phenotype of $Cc1^{-/-}$ mice (23), this impaired insulin clearance and caused hyperinsulinemia, hepatic insulin resistance, and features of fatty liver disease. Conversely, gain-of-function of hepatic CEACAM1 markedly reduced hyperinsulinemia, insulin resistance, and hepatic fat accumulation in response to prolonged HF intake. This is consistent with the notion that

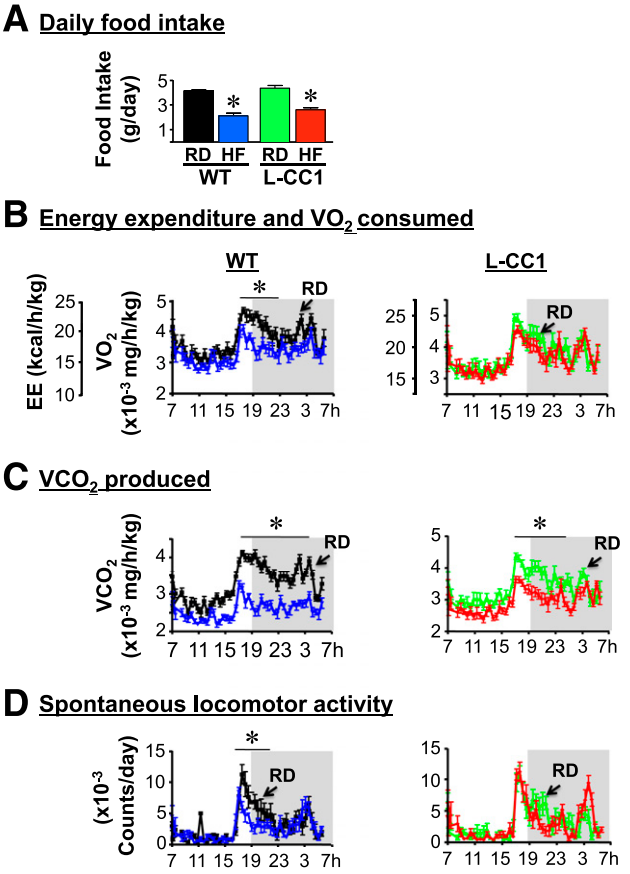

Figure 6—Indirect calorimetry analysis. WT (left) and L-CC1 mice (right) were fed RD (black or green) or HF diet (blue or red) for 4 months before being individually caged (n = 4 per feeding group per genotype), given free access to food, and subjected to indirect calorimetry analysis in a 24-h period for 5 days to measure daily food intake (*A*), heat production (energy expenditure [EE]) (kcal/h/kg lean mass) and VO_2 consumption (mg/h/kg lean mass) (*B*), VCO_2 production (mg/h/kg lean mass) (*C*), and spontaneous locomotor activity (counts/day) (*D*). Values are expressed as mean ± SEM of each time interval in the last 3 days. *P < 0.05 HF-fed vs. RD-fed per mouse group.

hyperinsulinemia caused by impaired insulin clearance can play a significant role in diet-induced insulin resistance and nonalcoholic fatty liver disease.

Our finding of a progressive increase in fat mass beginning at ~9 days of HF intake, followed by hyperinsulinemia and insulin resistance, agrees with previous reports (12,38). Schwartz and colleagues (12) showed that a 60% fat diet induced hyperinsulinemia in BL6 mice, before insulin resistance developed in liver and skeletal muscle (4–8 weeks) and subsequently in WAT (~14 weeks). This provided evidence of hyperinsulinemia preceding altered insulin signaling in peripheral insulin target tissues. Given that inducible liver-specific expression of CEACAM1 protected against hyperinsulinemia and insulin resistance in L-CC1 mice, we propose that the HF diet reduced hepatic CEACAM1 and, subsequently, impaired insulin clearance to alter insulin response in hepatocytes, followed by systemic insulin resistance.

That reduced insulin clearance plays a key role in diet-induced resistance agrees with previous reports in mice (39), dogs (40), and humans (41,42). Using a two-step hyperinsulinemic-euglycemic clamp, human studies (42) implicated reduction in insulin clearance in the rapid emergence of hepatic insulin resistance in young and healthy South Asian men, but not in Caucasians, after 5 days of an HF Western diet. This altered hepatic insulin clearance occurred in the absence of other differences in the metabolic and biochemical responses in skeletal muscle and WAT among both groups (42).

Inducible CEACAM1 expression in the liver increased fatty acid β-oxidation under both feeding conditions. This is likely due, at least partly, to higher hepatic FGF21 production and release (34,43). Of note, the HF diet induced fatty acid oxidation (FAO) in the WT and L-CC1 mice despite reducing FGF21 production relative to the RD. This points to an additional mechanism mediating FAO, likely mediated by direct ligand-dependent activation of peroxisome proliferator–activated receptor-α by "new fat" (44). The mechanism underlying the induction of FGF21 expression by CEACAM1 overexpression remains unknown, but that both proteins are induced by retinoic acid is intriguing (45,46). Further studies are needed to examine whether retinoic acid–related mechanisms mediate this correlation between hepatic CEACAM1 and FGF21 expression.

Overexpressing CEACAM1 in liver curtailed the negative effect of HF on locomotor activity and energy expenditure. Together with increased brown adipogenesis (47), increased activity could elevate energy dissipation. Given that CEACAM1 is not produced by adipose tissue, it is likely that extra-adipocytic mechanisms caused by hepatic CEACAM1 overexpression drove the increase in brown adipogenesis. This includes elevation in FGF21 release (36,37), which could induce locomotor activity (48). Although future studies are necessary to dissect the mechanisms involved in the regulation of physical activity and browning of adipose tissues by hepatic CEACAM1 induction, the L-CC1 response to the HF diet uncovers a putative novel role for hepatic CEACAM1 in regulating energy expenditure.

That reduction of CEACAM1-dependent mechanisms is implicated in diet-induced altered insulin and lipid metabolism is supported by our previous studies on rats selectively bred for low aerobic capacity. We have previously shown that hepatic CEACAM1 is markedly reduced in these rats relative to those with high aerobic capacity (49) and that caloric restriction, but not exercise, reversed hyperinsulinemia and insulin resistance in parallel to restoring hepatic CEACAM1 levels (50). Caloric restriction also reversed lipid accumulation and other features associated with nonalcoholic fatty liver disease in these rats with low aerobic capacity, including inflammation, oxidative stress, and fibrosis (50).

In summary, inducible CEACAM1 expression in liver restricted diet-induced insulin resistance by preserving insulin clearance and inducing hepatic β-oxidation and

energy dissipation. This provides a proof of principle that induction of CEACAM1 could curb the adverse metabolic effect of a HF diet.

Acknowledgments. The authors thank J. Kalisz and M. Kopfman at the Najjar Laboratory for their technical assistance in the generation, genotyping, and maintenance of mice, in addition to carrying out routine RNA and DNA analyses. The authors also thank Jiang Hu at the Kulkarni Laboratory for carrying out the immunohistochemistry analysis of pancreatic islets.

Funding. This work was supported by grants from the National Institutes of Health: R01-DK-67536 and R01-DK-103215 to R.N.K.; R01-DK-054254, R01-DK-083850, and R01-HL-112248 to S.M.N.; and U24-DK-093000 to the National Mouse Metabolic Phenotyping Center at University of Massachusetts. It was also partially supported by grants from the U.S. Department of Agriculture (USDA 38903-19826) to S.M.N.

Duality of Interest. No potential conflicts of interest relevant to this article were reported.

Author Contributions. Q.Y.A.-S. and S.G.L. researched data, designed experiments, and wrote the manuscript. A.M.D. researched data, designed and generated the targeting vector for the generation of the L-CC1 mouse line, screened and propagated the mouse line, and reviewed the manuscript. T.A.B., S.K.R., S.L.A., L.R., P.R.P., M.K.K., C.K.R., A.J.K., G.H., and A.D.L. researched data. J.K.K. carried out hyperinsulinemic-euglycemic clamp analysis and indirect calorimetry. R.N.K. carried out islet morphology experiments. W.M.P. generated the L-CC1 mouse. S.M.N. was responsible for study design, conceptualization, data analysis and results interpretation, and reviewing the manuscript. S.M.N. is the guarantor of this work and, as such, had full access to all the data in the study and takes responsibility for the integrity of the data and the accuracy of the data analysis.

References

1. Dankner R, Chetrit A, Shanik MH, Raz I, Roth J. Basal-state hyperinsulinemia in healthy normoglycemic adults is predictive of type 2 diabetes over a 24-year follow-up: a preliminary report. Diabetes Care 2009;32:1464–1466
2. Pories WJ, Dohm GL. Diabetes: have we got it all wrong? Hyperinsulinism as the culprit: surgery provides the evidence. Diabetes Care 2012;35:2438–2442
3. Corkey BE. Banting lecture 2011: hyperinsulinemia: cause or consequence? Diabetes 2012;61:4–13
4. Svedberg J, Björntorp P, Smith U, Lönnroth P. Free-fatty acid inhibition of insulin binding, degradation, and action in isolated rat hepatocytes. Diabetes 1990;39:570–574
5. Osborne TF. Sterol regulatory element-binding proteins (SREBPs): key regulators of nutritional homeostasis and insulin action. J Biol Chem 2000;275:32379–32382
6. Najjar SM, Russo L. CEACAM1 loss links inflammation to insulin resistance in obesity and non-alcoholic steatohepatitis (NASH). Semin Immunopathol 2014;36:55–71
7. Kabir M, Catalano KJ, Ananthnarayan S, et al. Molecular evidence supporting the portal theory: a causative link between visceral adiposity and hepatic insulin resistance. Am J Physiol Endocrinol Metab 2005;288:E454–E461
8. Scherer T, Lindtner C, Zielinski E, O'Hare J, Filatova N, Buettner C. Short term voluntary overfeeding disrupts brain insulin control of adipose tissue lipolysis. J Biol Chem 2012;287:33061–33069
9. Pereira S, Park E, Mori Y, et al. FFA-induced hepatic insulin resistance in vivo is mediated by PKCδ, NADPH oxidase, and oxidative stress. Am J Physiol Endocrinol Metab 2014;307:E34–E46
10. Chen S, Lam TK, Park E, et al. Oleate-induced decrease in hepatocyte insulin binding is mediated by PKC-delta. Biochem Biophys Res Commun 2006;346:931–937
11. Boden G. Fatty acid-induced inflammation and insulin resistance in skeletal muscle and liver. Curr Diab Rep 2006;6:177–181
12. Kim F, Pham M, Maloney E, et al. Vascular inflammation, insulin resistance, and reduced nitric oxide production precede the onset of peripheral insulin resistance. Arterioscler Thromb Vasc Biol 2008;28:1982–1988
13. Strissel KJ, DeFuria J, Shaul ME, Bennett G, Greenberg AS, Obin MS. T-cell recruitment and Th1 polarization in adipose tissue during diet-induced obesity in C57BL/6 mice. Obesity (Silver Spring) 2010;18:1918–1925
14. Lee YS, Li P, Huh JY, et al. Inflammation is necessary for long-term but not short-term high-fat diet-induced insulin resistance. Diabetes 2011;60:2474–2483
15. Meistas MT, Margolis S, Kowarski AA. Hyperinsulinemia of obesity is due to decreased clearance of insulin. Am J Physiol 1983;245:E155–E159
16. Jones CN, Abbasi F, Carantoni M, Polonsky KS, Reaven GM. Roles of insulin resistance and obesity in regulation of plasma insulin concentrations. Am J Physiol Endocrinol Metab 2000;278:E501–E508
17. Ader M, Stefanovski D, Kim SP, et al. Hepatic insulin clearance is the primary determinant of insulin sensitivity in the normal dog. Obesity (Silver Spring) 2014;22:1238–1245
18. Pivovarova O, Bernigau W, Bobbert T, et al. Hepatic insulin clearance is closely related to metabolic syndrome components. Diabetes Care 2013;36:3779–3785
19. Lee CC, Haffner SM, Wagenknecht LE, et al. Insulin clearance and the incidence of type 2 diabetes in Hispanics and African Americans: the IRAS Family Study. Diabetes Care 2013;36:901–907
20. Escobar O, Mizuma H, Sothern MS, et al. Hepatic insulin clearance increases after weight loss in obese children and adolescents. Am J Med Sci 1999;317:282–286
21. Formisano P, Najjar SM, Gross CN, et al. Receptor-mediated internalization of insulin. Potential role of pp120/HA4, a substrate of the insulin receptor kinase. J Biol Chem 1995;270:24073–24077
22. Poy MN, Yang Y, Rezaei K, et al. CEACAM1 regulates insulin clearance in liver. Nat Genet 2002;30:270–276
23. DeAngelis AM, Heinrich G, Dai T, et al. Carcinoembryonic antigen-related cell adhesion molecule 1: a link between insulin and lipid metabolism. Diabetes 2008;57:2296–2303
24. Xu E, Dubois MJ, Leung N, et al. Targeted disruption of carcinoembryonic antigen-related cell adhesion molecule 1 promotes diet-induced hepatic steatosis and insulin resistance. Endocrinology 2009;150:3503–3512
25. Najjar SM, Yang Y, Fernström MA, et al. Insulin acutely decreases hepatic fatty acid synthase activity. Cell Metab 2005;2:43–53
26. Lee W. The CEACAM1 expression is decreased in the liver of severely obese patients with or without diabetes. Diagn Pathol 2011;6:40
27. Walsh A, Ito Y, Breslow JL. High levels of human apolipoprotein A-I in transgenic mice result in increased plasma levels of small high density lipoprotein (HDL) particles comparable to human HDL3. J Biol Chem 1989;264:6488–6494
28. Kim JY, Koves TR, Yu GS, et al. Evidence of a malonyl-CoA-insensitive carnitine palmitoyltransferase I activity in red skeletal muscle. Am J Physiol Endocrinol Metab 2002;282:E1014–E1022
29. Heinrich G, Ghosh S, Deangelis AM, et al. Carcinoembryonic antigen-related cell adhesion molecule 2 controls energy balance and peripheral insulin action in mice. Gastroenterology 2010;139:644–652, e1
30. Taub M, Wang Y, Szczesny TM, Kleinman HK. Epidermal growth factor or transforming growth factor alpha is required for kidney tubulogenesis in matrigel cultures in serum-free medium. Proc Natl Acad Sci U S A 1990;87:4002–4006
31. Andrikopoulos S, Blair AR, Deluca N, Fam BC, Proietto J. Evaluating the glucose tolerance test in mice. Am J Physiol Endocrinol Metab 2008;295:E1323–E1332
32. Rader DJ. Molecular regulation of HDL metabolism and function: implications for novel therapies. J Clin Invest 2006;116:3090–3100
33. Najjar SM. Regulation of insulin action by CEACAM1. Trends Endocrinol Metab 2002;13:240–245

34. Inagaki T, Dutchak P, Zhao G, et al. Endocrine regulation of the fasting response by PPARalpha-mediated induction of fibroblast growth factor 21. Cell Metab 2007;5:415–425
35. Kunisch E, Fuhrmann R, Roth A, Winter R, Lungershausen W, Kinne RW. Macrophage specificity of three anti-CD68 monoclonal antibodies (KP1, EBM11, and PGM1) widely used for immunohistochemistry and flow cytometry. Ann Rheum Dis 2004;63:774–784
36. Emanuelli B, Vienberg SG, Smyth G, et al. Interplay between FGF21 and insulin action in the liver regulates metabolism. J Clin Invest 2014;124:515–527
37. Owen BM, Ding X, Morgan DA, et al. FGF21 acts centrally to induce sympathetic nerve activity, energy expenditure, and weight loss. Cell Metab 2014; 20:670–677
38. Park SY, Cho YR, Kim HJ, et al. Unraveling the temporal pattern of diet-induced insulin resistance in individual organs and cardiac dysfunction in C57BL/6 mice. Diabetes 2005;54:3530–3540
39. Liu J, Zhou L, Xiong K, et al. Hepatic cannabinoid receptor-1 mediates diet-induced insulin resistance via inhibition of insulin signaling and clearance in mice. Gastroenterology 2012;142:1218–1228, e1
40. Mittelman SD, Van Citters GW, Kim SP, et al. Longitudinal compensation for fat-induced insulin resistance includes reduced insulin clearance and enhanced beta-cell response. Diabetes 2000;49:2116–2125
41. Erdmann J, Kallabis B, Oppel U, Sypchenko O, Wagenpfeil S, Schusdziarra V. Development of hyperinsulinemia and insulin resistance during the early stage of weight gain. Am J Physiol Endocrinol Metab 2008;294:E568–E575
42. Bakker LE, van Schinkel LD, Guigas B, et al. A 5-day high-fat, high-calorie diet impairs insulin sensitivity in healthy, young South Asian men but not in Caucasian men. Diabetes 2014;63:248–258
43. Fisher FM, Chui PC, Nasser IA, et al. Fibroblast growth factor 21 limits lipotoxicity by promoting hepatic fatty acid activation in mice on methionine and choline-deficient diets. Gastroenterology 2014;147:1073–1083 e1076
44. Chakravarthy MV, Pan Z, Zhu Y, et al. "New" hepatic fat activates PPARalpha to maintain glucose, lipid, and cholesterol homeostasis. Cell Metab 2005;1:309–322
45. Pantelic M, Chen I, Parker J, Zhang P, Grunert F, Chen T. Retinoic acid treated HL60 cells express CEACAM1 (CD66a) and phagocytose Neisseria gonorrhoeae. FEMS Immunol Med Microbiol 2004;42:261–266
46. Li Y, Wong K, Walsh K, Gao B, Zang M. Retinoic acid receptor β stimulates hepatic induction of fibroblast growth factor 21 to promote fatty acid oxidation and control whole-body energy homeostasis in mice. J Biol Chem 2013;288:10490–10504
47. Rosenbaum M, Leibel RL. Leptin: a molecule integrating somatic energy stores, energy expenditure and fertility. Trends Endocrinol Metab 1998;9:117–124
48. Cornu M, Oppliger W, Albert V, et al. Hepatic mTORC1 controls locomotor activity, body temperature, and lipid metabolism through FGF21. Proc Natl Acad Sci U S A 2014;111:11592–11599
49. Wisløff U, Najjar SM, Ellingsen O, et al. Cardiovascular risk factors emerge after artificial selection for low aerobic capacity. Science 2005;307:418–420
50. Bowman TA, Ramakrishnan SK, Kaw M, et al. Caloric restriction reverses hepatic insulin resistance and steatosis in rats with low aerobic capacity. Endocrinology 2010;151:5157–5164